Microbiota-Derived Indole Metabolites Promote Human and Murine Intestinal Homeostasis through Regulation of Interleukin-10 Receptor

Alexeev, E. E., Lanis, J. M., Kao, D. J., Campbell, E., Kelly, C. J., Battista, K. D., Gerich, M. E., Jenkins, B. R., Walk, S. T., Kominsky, D. J., & Colgan, S. P. (2018). Microbiota-Derived Indole Metabolites Promote Human and Murine Intestinal Homeostasis through Regulation of Interleukin-10 Receptor. *The American journal of pathology*, *188*(5), 1183-1194. https://doi.org/10.1016/j.ajpath.2018.01.011

Published in:
The American journal of pathology

Document Version:
Peer reviewed version

Microbiota-derived indole metabolites promote human and murine intestinal homeostasis through regulation of interleukin-10 receptor

Short title: Indole metabolites and intestinal homeostasis

Erica E. Alexeev[1], Jordi M. Lanis[1], Daniel J. Kao[1], Eric L. Campbell[2], Caleb J. Kelly[1], Kayla D. Battista[1], Mark E. Gerich[1], Brittany R. Jenkins[3], Seth T. Walk[3], Douglas J. Kominsky[3#], Sean P. Colgan[1#]

[1]*Mucosal Inflammation Program and Department of Medicine, University of Colorado, Anschutz Medical Campus, Aurora, CO*

[2]*Centre for Experimental Medicine, Queen's University Belfast, Belfast, BT97BL, Northern Ireland, UK*

[3]*Department of Microbiology and Immunology, Montana State University, Bozeman, MT*

[#]*Co-senior authors*

Funding: This work was supported by NIH grants DK1047893, DK50189, DK095491, DK103639, DK103712 and VA Merit BX002182. Funding for generating and maintaining the human intestinal organoids was provided by the Bill and Melinda Gates Foundation.

Correspondence to: Sean Colgan, Mucosal Inflammation Program, University of Colorado, Anschutz Medical Campus, 12700 East 19th Ave. MS B-146, Aurora, CO 80045, USA. Office phone: 303-724-7235 Fax: 303-724-7243
E-mail: sean.colgan@ucdenver.edu
or
Douglas Kominsky, Department of Microbiology and Immunology, Montana State University, 109 Lewis Hall, Bozeman, MT 59717, USA. Office phone: 406-994-5667 Fax: 406-994-4926
E-mail: douglas.kominsky@montana.edu

Competing interests: The authors declare that no conflict of interests exists.

Abstract

Interactions between the gut microbiota and the host are important for health, where dysbiosis has emerged as a likely component of mucosal disease. The specific constituents of the microbiota that contribute to mucosal disease are not well defined. We sought to define microbial components that regulate homeostasis within the intestinal mucosa. Using an unbiased, metabolomic profiling approach, we identified a selective depletion of indole and indole-derived metabolites in murine and human colitis. We demonstrated that indole-3-propionic acid (IPA) was selectively diminished in circulating serum from human subjects with active colitis and that IPA served as a biomarker of disease remission. Administration of indole metabolites showed prominent induction of IL-10R1 on cultured intestinal epithelia that was explained by activation of the aryl hydrocarbon receptor (AHR). Colonization of germ-free mice with wild-type *E. coli*, but not *E. coli* mutants unable to generate indole, induced colonic epithelial IL-10R1. Moreover, oral administration of IPA significantly ameliorated disease in a chemically-induced murine colitis model. This work defines a novel role of indole metabolites in anti-inflammatory pathways mediated by epithelial IL-10 signaling and identifies possible avenues for utilizing indoles as novel therapeutics in mucosal disease.

Keywords: indole; microbiota; colitis; mucosal homeostasis

48 **Introduction**

49 The mammalian gastrointestinal (GI) tract plays host to trillions of microbes, collectively termed
50 the microbiota, where a critical mutualism exists within the intestinal mucosa. The microbiota contributes
51 significantly to gut homeostasis but can also contribute to establishing and maintaining mucosal disease [1].
52 Intestinal mucosal surfaces act as primary barriers to microbial invasion, where commensal bacteria work
53 in a dynamic and intimate interaction with the gut epithelium and influence host cellular and immune
54 responses [2]. Inflammatory bowel disease (IBD) is a chronic inflammatory disease of the GI tract that is
55 comprised of Crohn's disease (CD) and ulcerative colitis (UC). It is known that IBD is caused by
56 interactions between genetic and environmental factors, and results in perturbations of the microbiota,
57 though precisely how microbial factors affect gut homeostasis and immune response have not been
58 extensively explored [3-5].

59 The significance of IL-10 signaling is well established in IBD. This anti-inflammatory cytokine,
60 which signals through the IL-10 receptor ligand-binding subunit (IL-10R1), is induced during
61 inflammation and attenuates excessive production of pro-inflammatory mediators in various cell types,
62 including intestinal epithelial cells (IEC) [6, 7]. Functional IL-10 signaling is associated with enhanced
63 mucosal barrier function and results in maintenance and homeostasis of the epithelia [7]. Previous work,
64 including our own, has shown that the epithelial IL-10R1 contributes fundamentally to resistance to
65 intestinal inflammation and represents a component of epithelial innate immunity originally described to
66 be induced by cytokines such as IFN-γ[8]. For instance, mice deficient in IL-10 or IL-10 receptor develop
67 spontaneous severe colitis and mice conditionally lacking intestinal epithelial IL-10R1 show increased
68 susceptibility to colitis [7, 9, 10].

69 Metabolomic analysis has revealed that gut bacteria impact host immunity through a variety of
70 metabolites, including indole metabolites [11], which originate from the microbial metabolism of
71 tryptophan. Indole-3-propionic acid (IPA) and indole-3-aldehyde (IAld), which are tryptophan
72 metabolites produced by intestinal bacteria, are known for their intercellular signaling activity. Further,

73 IAld has recently been identified as an aryl hydrocarbon receptor (AHR) ligand [12]. AHR is a ligand-
74 dependent transcription factor activated by a variety of synthetic and biological molecules that plays an
75 important role in immunological response and inhibition of inflammation [13]. AHR contributes to immune
76 homeostasis through various methods, including T cell differentiation and Th17 development [14, 15], as well
77 as the upregulation of IL-22 production [16]. Recently, several studies have shown that the host microbiota
78 provides a consistent source of endogenous AHR ligands with distinct effects on immune homeostasis [16-
79 18]. However, the precise role of indole metabolites in the gastrointestinal tract remains elusive. Together,
80 these data lead us to hypothesize that microbial-derived indole metabolites promote intestinal homeostasis
81 through AHR-mediated regulation of the IEC IL-10R1.
82
83
84
85
86
87
88
89
90
91
92
93
94
95
96

97 **Materials and Methods**

98 **Animal Studies**

99 For metabolomics analysis, C57BL/6-129 mice were administered 3% (wt/vol) dextran sodium sulfate
100 (DSS; molecular weight 36,000-50,000; MP Biochemicals, Burlingame, CA) in drinking water for 5 d,
101 followed by a 2-d recovery period. Normal tap water was returned during these 2 d prior to tissue
102 collection. Control mice were maintained on tap water for 7 d. In subsequent animal experiments, 8-12
103 wk-old C57BL/6 mice were administered water or 2.5% DSS *ad libitum* for 9 d. This administration
104 approach varied slightly to account for a change in death susceptibility to DSS. DSS was then removed
105 and mice were allowed to recover for 2 d prior to euthanasia. For IPA treatment experiments, the addition
106 of IPA at 0.1 mg/ml was administered to water- and DSS-treated animals. Mice were housed in
107 accordance with guidelines from the American Association for Laboratory Animal Care and Research
108 Protocols, and all animal work was approved by the Institutional Animal Care and Use Committee of the
109 University of Colorado. 10mg in 103ml DI H2O

110

111 **Cell Lines and shRNA Knockdown**

112 Human T84 intestinal epithelial cells (IEC) were cultured in 1:1 DMEM-Ham's F12 with 2.5 mM L-
113 glutamine and 10% FBS. Cells were maintained at 37°C with 5% CO_2. Transepithelial electrical
114 resistances (TEER) were monitored using an EVOM2 Voltohmmeter (World Precision Instruments,
115 Sarasota, FL). Cytokines were purchased from R&D Systems (Minneapolis, MN). IAld, IPA, and AHR
116 inhibitor, CH-223191, were obtained from Sigma Aldrich (St. Louis, MO). 6-formylindole[3,2-b]
117 carbazole (FICZ) was obtained from Tocris Bioscience (Bristol, United Kingdom). All compounds were
118 used at indicated concentrations. Human intestinal organoids (HIOs) were derived following previously
119 described methods [19] and kindly provided by Dr. Jason Spence at the University of Michigan. HIOs were
120 maintained by embedding in Matrigel (BD Biosciences) and applying Advanced DMEM-F12 medium
121 (Invitrogen, Carlsbad, CA) containing 1X B27 supplement (Invitrogen), 1X GlutaMAX (Life
122 Technologies, Carlsbad, CA), 10 μM Hepes, 10% pen/strep, 100 ng/mL rhNoggin (R&D Systems), 100

123 ng/mL epidermal growth factor (R&D Systems), and approximately 500 ng/mL R-Spondin1 (RSPO1).
124 RSPO1 was obtained from conditioned media collected from a HEK293 cell line that was stably
125 transfected and zeocin-selected for the RSPO1 expression vector. Media was changed every two to four
126 days, and HIOs were transferred to fresh Matrigel once a week until they reached approximately 0.5 mm
127 to 1 mm in size for experiments and RNA isolation. Lentiviral particles encoding shRNA directed against
128 ARNT (MISSION TRC shRNA, University of Colorado Functional Genomics Facility) were used to
129 transduce T84 cells using standard protocols. Stable integration was achieved by puromycin selection at 6
130 µg/ml. Knockdown was confirmed by qPCR analysis, indicating 80-85% depletion of ARNT levels.
131
132 **RNA Isolation and Real-Time PCR**
133 Total RNA was extracted from cells using TRIzol (Invitrogen) and from tissue using RNeasy Mini Kit
134 (Qiagen, Hilden Germany). cDNA was prepared using iScript cDNA synthesis kit (Bio-Rad, Hercules,
135 CA). Real-time PCR to measure transcript was carried out in 1× Power SYBR Green master mix (Applied
136 Biosystems, Foster City, CA) using an ABI 7300 thermocycler. Fold change in expression of target
137 mRNA relative to β-actin mRNA was calculated as previously described [20]. Total RNA from HIOs was
138 isolated using Direct-zol RNA Miniprep Kit (Zymo Research Corp, Irvine, CA). Fold change in
139 expression of mRNA transcript from HIO experiments was calculated relative to HSPCB (heat shock
140 protein 90 alpha family class B member 1). Human and mouse primer sequences listed in Table 1.
141
142 **Western Blot**
143 Whole cell and tissue lysates was extracted in Tris-Lysis buffer on ice and disrupted by sonication.
144 Protein content was quantified using BCA protein assay reagent (Thermo Scientific, Waltham, MA) and
145 30 µg of whole cell or tissue extract was boiled in Laemmli buffer in reducing conditions subjected to
146 SDS/PAGE. The SDS/PAGE was transferred onto a PVDF membrane and probed for IL-10R1 using a
147 rabbit polyclonal IL-10RA antibody (1: 1000; Thermo Fisher, Waltham, MA) and β-actin (1: 10,000;
148 Abcam, Cambridge, UK).

149

150 **Metabolomic Analysis**

151 Distal colon tissue (1 cm) was collected from control and DSS-treated mice. Tissues were flash frozen
152 and placed at -80˚C. Global metabolomics was performed by Metabolon, Inc. (Durham, NC). Briefly,
153 tissue samples were thawed and weighed in tared cryovials and 80% ice-cold methanol was added at a
154 ratio of 75µL solvent per mg of sample, then incubated overnight at 4˚C to extract biochemicals. Internal
155 standards were included to control for extraction efficiency. Following methanol extraction, colon
156 samples were processed and analyzed as previously described [21].

157

158 **HPLC Metabolite Analysis**

159 Indole derivatives were quantified in mouse and human samples using reversed-phase high-performance
160 liquid chromatography with electrochemical coulometric array detection (EC-HPLC; CoulArray, Thermo
161 Scientific, Waltham, MA). Archived human serum samples from patients diagnosed with IBD or from
162 healthy individuals were obtained under research protocols approved by the Colorado Multi-Institutional
163 Review Board. Study participant demographics are listed in Table 2. Tissue and serum samples were
164 extracted in 80% methanol and protein precipitate was removed by centrifugation at 15,000 x *g*.
165 Separation was achieved using an Acclaim Polar Advantage II C18 column (Thermo, Waltham, MA) at a
166 flow rate of 1 ml/min on a gradient of 10% to 55% acetonitrile in 50 mM sodium phosphate buffer, pH 3,
167 containing 0.42 mM octanesulphonic acid as an ion-pairing agent. Calibration curves were composed by
168 performing linear regression analysis of the peak area versus the analyte concentration. The data were
169 quantified using the peak area in comparison to standards.

170

171 **Bacterial Strains and Gnotobiotic Colonization Experiments**

172 *Escherichia coli* (*E. coli*) strains were obtained from GE Dharmacon (Lafayette, CO). An *E. coli* K12
173 parent strain (*E. coli* BW25113; *WT)*, along with strains containing a deletion of *tnaA* (*E. coli JW3686*;
174 Δ*tnaA*) and *tnaB* (*E. coli* JW5619; Δ*tnaB*) were used for experiments. All strains were grown in Lysogeny

175 broth (LB; 10g/L tryptone, 10g/L NaCl, 5 g/L yeast extract) or on LB-agar plates supplemented with
176 appropriate antibiotics (kanamycin, 50 µg/ml), if needed. Cultures were grown overnight at 37˚C to
177 stationary phase and tested for the presence of indole by the addition of 200 µL of Kovac's reagent
178 (Sigma Aldrich, St. Louis, MO) to 2 mL bacterial culture. For T84 cell experiments, cultures were grown
179 overnight at 37˚C to stationary phase. Briefly, cultures were spun, supernatants collected, and afterward
180 serially diluted and placed onto cells for 24 hr. Bacterial supernatants used for EC-HPLC analysis were
181 placed through a 0.22 µm filter prior to run. For gnotobiotic colonization experiments, 5-8-week-old
182 germ-free C57BL/6 mice were gavaged with a 100 µL bacterial suspension for mono-association (10^9
183 CFU of each bacterial strain collected from a stationary-phase culture and re-suspended in PBS). Mice
184 were colonized for 2 wk prior to euthanasia. Fresh fecal pellets were collected periodically, weighed,
185 homogenized and serially diluted in PBS for plating to determine bacterial CFU per g of feces.
186
187 **Histology**
188 Colon samples were fixed in 10% neutral buffered formalin and paraffin embedded prior to staining with
189 hematoxylin and eosin (H&E). All histological quantitation was performed blinded by the same individual
190 using a scoring system previously described [22]. Briefly, the three independent parameters measured were
191 severity of inflammation (0–3: none, slight, moderate, severe), extent of injury (0–3: none, mucosal,
192 mucosal and submucosal, transmural), and crypt damage (0–4: none, basal 1/3 damaged, basal 2/3
193 damaged, only surface epithelium intact, entire crypt and epithelium lost). The score of each parameter
194 was multiplied by a factor reflecting the percentage of tissue involvement (x1: 0–25%, x2: 26–50%, x3:
195 51–75%, x4: 76–100%) and all numbers were summed. Maximum possible score was 40.
196
197 **Quantification of Cytokines in Colon Tissue**
198 For cytokine analysis, colon tissue was extracted in Tris-Lysis buffer by sonication and protein
199 homogenates were quantified using BCA protein assay reagent (Thermo Scientific, Waltham, MA).
200 Tissue concentrations of cytokines were measured using a proinflammatory cytokine screen (Meso Scale

201 Discovery, Rockville, MD). Assays were performed according to manufacturer's instructions. Cytokine
202 concentrations were normalized to total protein concentration.
203
204 **Quantification and Statistical Analysis**
205 Data are expressed as mean ± S.E.M. Statistical analyses were performed in GraphPad Prism (La Jolla,
206 CA, Version 7.0) using two-tailed unpaired Student's *t*-test for direct comparisons and one-way or two-
207 way ANOVA with Tukey's test for multiple comparisons. Statistical differences reported as significant
208 when $P < 0.05$.
209
210
211
212
213
214
215
216
217
218
219
220
221
222
223
224

225 **Results**

226 **Tryptophan-indole metabolism is altered in murine and human colitis**

227 To better understand microbe-derived factors that contribute to intestinal homeostasis, we
228 performed a comprehensive, unbiased screen of serum and colonic tissue metabolites from healthy and
229 DSS colitic mice. Mice were administered DSS via drinking water, and serum and colonic tissue were
230 collected during peak disease (day 7). Of the microbe-derived metabolites, most notable were decreases in
231 tryptophan-indole metabolites in both serum and colons of colitic mice compared to mice administered
232 water alone (Figure 1A). Tryptophan is metabolized through various pathways, including the indole
233 pathway, resulting in derivatives that are produced from metabolism by gut microbiota (Figure 1B).
234 Colitis profoundly altered tryptophan metabolism, specifically revealing a selective decrease in indole
235 metabolites. To validate this mass spectrometry-based metabolite screen, we developed an HPLC-based
236 protocol using electrochemical (EC) detection methods (Figure 1C). Eight- to ten-week-old C57BL/6
237 mice were administered water or 2.5% DSS *ad libitum* for 9 d. DSS was then removed and mice were
238 allowed to recover for 2 d prior to euthanasia. Serum indole metabolites were profiled by EC-HPLC
239 (Figure 1D). Serum indole and IPA levels were significantly decreased in actively colitic animals ($P <$
240 0.05). A marked decrease in serum IAld was also observed ($P = 0.09$). It is notable that overall tryptophan
241 levels in DSS colitis actually increase (Figure 1A), suggesting that our findings of indole depletion are not
242 a result of diminished tryptophan absorption.

243 Guided by results of indole depletion in active murine colitis, we attempted to translate our results
244 to human patients. Here, we used our developed EC-HPLC method to quantify various indole metabolites
245 in serum samples from patients with UC. For these purposes, serum samples from healthy controls (n =
246 20), subjects with active UC (n = 15), and subjects with UC in remission (n = 20) were profiled (see
247 Table 2 for demographics). This analysis revealed that serum IPA was deceased by nearly 60% in
248 subjects with active UC compared to healthy controls ($P < 0.05$, Figure 1E). Notably, this IPA deficiency
249 normalized in UC patients in remission, implicating IPA as both a biomarker for active UC as well as an

250 indicator of disease remission in human UC. Based on these findings, we further explored the role of
251 indole and metabolites IPA and IAld on intestinal epithelial function.
252
253 **Indole metabolites induce IL-10R1 expression on intestinal epithelia and improve barrier formation**
254 We have previously shown that tryptophan metabolites are important regulators of IL-10R1 in
255 IEC [23]. Guided by our unbiased metabolomic profile of serum and colon tissue from healthy and DSS-
256 colitic mice and our recent work identifying the epithelial interleukin-10 receptor as the dominant
257 signature for resolution of inflammation in DSS colitis[6, 7], we hypothesized that indole-containing
258 tryptophan metabolites regulate intestinal homeostasis via regulation of epithelial IL-10R1 expression. To
259 examine the induction of IL-10R1 in response to indole metabolites, T84 IEC were exposed to IPA or
260 IAld for 6 h. qPCR of IL-10R1 transcript levels showed a concentration-dependent induction of IL-10R1
261 (Figure 2A). These findings were not limited to colonic cancer cell lines. Human intestinal organoids
262 (HIOs) are complex three-dimensional spheroid tissues derived from human pluripotent stems cells
263 (hPSCs) [19] and contain the majority of functional epithelial cell types (i.e. enterocytes, goblet, Paneth,
264 enteroendocrine, intestinal stem cells) and structures (i.e. brush borders of microvilli, crypt-like
265 structures, and a mesoderm layer) comprising the human small intestine [24]. HIOs treated with IPA
266 exhibited increasing levels of IL-10R1 transcript, with significant induction at 24 h ($P < 0.001$; Figure
267 2B). Further analysis revealed a prominent induction of IL-10R1 protein expression in T84 IEC exposed
268 to IPA and IAld (Figure 2C).
269 We next examined the influence of the metabolite IAld on barrier formation in T84 cell
270 monolayers, as our previous work has demonstrated that IL-10 signaling is important in IEC barrier
271 development and maintenance [7, 23]. Cells exposed to both IAld and IL-10 exhibited significantly increased
272 barrier formation at 72 h compared with untreated cells as measured by TEER ($P < 0.01$; Figure 2D).
273 Further, IAld in combination with IL-10 (10ng/ml) significantly induced Suppressor of Cytokine
274 Signaling 3 (SOCS3), an IL-10-responsive gene that has been found to be protective in intestinal
275 inflammation [25] ($P < 0.05$; Figure 2E). From this perspective, it is notable that SOCS3 was not induced by

276 IL-10 alone as a result of nearly undetectable levels of IL-10R1 at baseline [6, 7]. Overall, these results
277 identify indole metabolite-dependent induction of the epithelial IL-10R1 as a target pathway for mucosal
278 homeostasis.
279
280 **Loss of indole-dependent IL-10R1 induction in cells lacking ARNT**
281 We next sought to define the mechanism of indole signaling in intestinal epithelia. Others have
282 shown that tryptophan metabolites function as endogenous ligands for AHR [26]. To determine the relative
283 contribution of AHR to indole signaling, we utilized short hairpin RNA knockdown to deplete the AHR
284 dimeric partner ARNT and examined IL-10R1 induction as an endpoint. Lentiviral shRNA-mediated
285 knockdown of ARNT (shARNT) in T84 IEC resulted in significantly reduced ARNT mRNA expression
286 (81 ± 5% decrease, $P < 0.01$) relative to cells containing a non-template control (shNTC) (Figure 3A). A
287 broader examination of classical AHR-ARNT target genes [26-28] revealed that transcript levels of CYP1A1
288 and CYP1B1 were significantly increased in shNTC cells treated with IAld compared to untreated shNTC
289 cells. Both targets were also significantly increased in the IAld-treated shNTC compared to shARNT T84
290 IEC following IAld treatment ($P < 0.01$, $P < 0.05$, respectively; Figure 3B). Analysis of these ARNT-
291 deficient cells revealed a prominent decrease in IAld-dependent induction of IL-10R1 transcript and
292 protein ($P < 0.05$; Figures 3C-E). The AHR small-molecule inhibitor, CH-223191, serves as a specific
293 AHR antagonist. shNTC and shARNT T84 IEC were exposed to IAld (1mM), CH-223191 (10μM), or in
294 combination for 24 h. IAld treatment alone significantly increased IL-10R1 expression at 24 h. CH-
295 223191 significantly reduced IAld-mediated IL-10R1 induction, supporting our hypothesis that IAld
296 modulates IL-10R1 expression via an AHR-mediated mechanism ($P < 0.05$, Figure 3F). These results
297 suggest that the AHR pathway is involved in the indole metabolite-dependent expression of IL-10R1 in
298 IEC.
299
300 **Bacterial indole production induces IL-10R1**

301 We next sought to determine whether microbe-derived sources of indole could similarly regulate
302 epithelial target genes. For these purposes, we targeted indole production in *Escherichia coli* (*E. coli*).
303 Indole is synthesized from tryptophan by microbial tryptophanase [29]. Using Kovac's reagent to test for the
304 presence of indole, we show that an *E. coli* K12 strain (*E. coli* BW25113; *WT*) clearly produced indole
305 (Figure 4A), whereas deletion of the tryptophanase gene *(*Δ*tnaA)* revealed a lack of detectable indole.
306 Conversely, deletion of one of the tryptophan transporters *(*Δ*tnaB*) does not compromise indole
307 production (Figure 4A). To validate these observations, the presence of indole in cell-free supernatants of
308 bacteria was examined by EC-HPLC. While *E. coli WT* bacteria exhibited readily detectable levels of
309 indole, metabolism of tryptophan to indole was completely abolished in *E. coli* Δ*tnaA* (Figure 4B). To test
310 the activity of this microbial-derived indole, cell-free supernatants from *E. coli WT* and Δ*tnaA* mutant
311 were serially diluted and exposed to T84 IEC for 24 h. Supernatants from *E. coli WT* readily induced IL-
312 10R1 protein expression, while minimal IL-10R1 induction was observed in cells exposed to *E. coli*
313 Δ*tnaA* supernatant (Figure 4C).
314 We extended these findings to an *in vivo* model. Herein, we examined the function of indole-
315 producing bacteria on epithelial IL-10R1 in germ-free mice. Germ-free mice were colonized with *E. coli*
316 *WT* or *E. coli* Δ*tnaA* for 2 wk followed by euthanasia. Fresh fecal pellets were collected periodically for
317 plating to ensure equal colonization, quantified as bacterial CFU per g of feces (data not shown). Indole
318 concentrations in cecal contents were validated by HPLC in vehicle and colonized animals. Mice
319 monocolonized with *E. coli WT* displayed significantly increased cecal indole, while negligible levels
320 were measured in PBS- and *E. coli* Δ*tnaA*-gavaged animals ($P < 0.01$; Figure 4D). Further, colons were
321 harvested and RNA extracted for qPCR analysis. This strategy revealed that mice monocolonized with *E.*
322 *coli WT* displayed significantly increased colonic *il10r1* expression, while no significant *il10r1* induction
323 was observed in colon tissue of mice colonized with *E. coli* Δ*tnaA* mutant ($P < 0.05$; Figure 4E). Taken
324 together, these *in vitro* and *in vivo* results strongly support our hypothesis that microbe-derived indoles
325 promote epithelial homeostasis.
326

327 **IPA improves DSS colitis outcomes**

328 Given the observation that indole metabolites are significantly decreased in active colitis, we
329 tested the therapeutic potential of IPA in murine colitis outcomes. For these purposes, mice were
330 administered either normal drinking water, DSS (2.5% wt/vol) or a combination of DSS and IPA (0.1
331 mg/ml) in drinking water for 9 d, followed by DSS removal and a 2-d recovery. To verify that oral
332 administration normalized IPA levels, colonic IPA was quantified by EC-HPLC. This analysis revealed
333 that while DSS colitic mice displayed significantly lower levels of IPA, oral administration of IPA
334 normalized colonic levels of this metabolite ($P < 0.01$; Figure 5A). Under these treatment conditions,
335 DSS/IPA-treated animals displayed significantly less reduction in colon length, a marker of intestinal
336 inflammation, compared to DSS-treated animals ($P < 0.05$; Figure 5B). Histological analysis revealed that
337 DSS/IPA-treated mice displayed attenuated inflammatory infiltration and decreased loss of architecture in
338 comparison to mice treated with DSS alone, which displayed pronounced loss of epithelium and tissue
339 architecture (Figure 5C). These differences resulted in greater histopathological severity scores ($P <$
340 0.001; Figure 5D). We additionally examined tissue cytokine levels in these mice. Pro-inflammatory
341 cytokine levels were dramatically increased in DSS-treated mice, specifically IFN-γ ($P < 0.05$; Figure
342 5E), TNF-α ($P < 0.01$; Figure 5F), and IL-1β ($P < 0.05$; Figure 5G), while cytokine levels in DSS/IPA-
343 treated mice were similar to mice administered water alone. Similarly, IL-10 levels were significantly
344 increased in DSS-treated mice, though IPA administration did not alter levels of this cytokine
345 (Supplemental Figure S1). Further, IPA administration increased transcript and protein levels of AHR
346 target genes (Supplemental Figure S2). Taken together, these results indicate that therapeutic
347 normalization of IPA during active colitis attenuates disease and promotes intestinal homeostasis.
348
349
350
351

352 **Discussion**

353 Recent efforts to define the complex nature of IBD have focused on the contribution of the host
354 microbiota. It is now established that altered microbial composition, termed dysbiosis, is strongly
355 associated with IBD [30] and other intestinal diseases [31]. Such dysbiosis is thought to alter the immune
356 response and influence epithelial function, resulting in increased intestinal permeability [32]. The particular
357 components of the microbiome that promote disease and distinguish phenotypes are not well understood.
358 In the current work, we sought to identify and characterize microbial-derived metabolites that contribute
359 to colonic disease and homeostasis.

360 Immunometabolism is an area of significant interest in mucosal inflammation [33]. Guided by an
361 unbiased metabolomic profile of serum and colon tissue from healthy and DSS-colitic mice, we identified
362 a significant shift in tissue-associated, microbiota-derived indole derivatives. We show that tryptophan
363 does not decrease in murine colitis. In fact, tryptophan levels significantly increased in colons of colitic
364 mice. Based on these findings, we believe the observed decrease of indole metabolites to be a result of a
365 selective depletion of tryptophan-indole metabolites due to dysbiosis, rather than poor absorption of
366 tryptophan.

367 Indole is produced from the action of microbial tryptophanase on tryptophan to produce indole,
368 pyruvate, and ammonia via a β-elimination reaction [34]. Microbes that express tryptophanase have the
369 capacity to utilize tryptophan as a source of nitrogen, carbon, and energy [35]. The *tnaA* gene, encoding
370 tryptophanase, is highly conserved among Gram-negative indole-producing species including
371 *Citrobacter*, *Morganella*, *Klebsiella*, *Providencia*, and *Haemophilus influenzae* type b [36]. The presence of
372 *tnaA* is strongly associated with virulence of *H. influenzae* [37]. At present, we do not know the nature of
373 indole deficiencies associated with active inflammation, though our work is consistent with a study
374 demonstrating that bacterial fermentation metabolites are less abundant in patients with IBD compared
375 with healthy controls [38]. Additionally, Wlodarska et al. have recently shown that microbes of IBD patients
376 have a reduced ability to cleave intestinal mucins and metabolize tryptophan [39]. Such a precedent exists
377 for other microbiota-derived metabolites. For example, studies investigating dysbiosis in IBD have

378 identified lower concentrations of luminal short chain fatty acids (SCFA) and significant depletion of
379 butyrate-producing organisms (e.g., specific *Faecalibacterium* and *Roseburia* genera) with active colonic
380 disease [40-42]. It is therefore likely that our observed decreases in indole metabolism reflect inflammation-
381 associated dysbiosis.

382 Some evidence exists that microbial-derived indole and indole metabolites could be anti-
383 inflammatory. For instance, Shimada *et. al.* demonstrated that indole administration to germ-free mice
384 increased the expression of some epithelial tight junction proteins and attenuated weight loss in a DSS
385 colitis model [43]. No mechanisms were evaluated to describe these changes elicited by indole. Moreover,
386 Venkatesh et al. have shown that IPA is a ligand for the pregnane X receptor (PXR) and promotes
387 intestinal barrier integrity through down-regulation of epithelial TNFα, induction of MDR1, and
388 regulation of epithelial junctional complexes [44]. It is interesting to note that PXR, a member of the
389 superfamily of nuclear receptors, is under consideration as a novel drug target in IBD [45]. Further,
390 Wlodarska et al. have shown that the metabolite indoleacrylic acid promotes intestinal barrier function
391 and mitigates inflammatory responses through downregulation of genes involved in inflammation and
392 oxidative stress [39]. Conversely, it is also notable that some indole derivatives have also been shown to be
393 nephrotoxic. For example, Devlin et al. recently identified a widely distributed family of tryptophanases
394 produced by commensal *Bacteroides* within in the gut microbiota [46]. They demonstrate that microbe-
395 derived indoles are modified by the host to generate toxic renal levels of indoxyl sulfate and that
396 colonization with tryptophanase-deficient *Bacteroides* decreases systemic levels of indoxyl sulfate that
397 may be renal protective.

398 We translated these findings of shifts in indole metabolism from murine colitis to human subjects.
399 This analysis revealed, for the first time, that serum indole metabolites in human subjects with active UC
400 revealed a remarkable similarity to mice with active colitis, with the exception that human subjects were
401 selectively deficient in IPA and not indole or IAld. The reason for this selective loss of IPA in humans is
402 not known. It should be noted that indole and indole metabolites are produced by different pathways and
403 different bacteria. Since IPA is an indole derivative conjugated to propionate and propionate is among the

404 SCFAs that become depleted in active human IBD [47], it is possible that this selective depletion of IPA is
405 explained by an IBD-associated dysbiosis that results from the combined depletion of both SCFA- and
406 indole-producing microbiota. Further studies will be necessary to define the nature of this observation.
407 Therapeutic administration of oral IPA was protective in a murine model of colitis. Animals that
408 received IPA not only exhibited fewer physical signs of disease, but also had significantly less damage to
409 crypt structure and restricted inflammatory infiltration. Indoles and other tryptophan metabolites have been
410 demonstrated to function as AHR ligands [26, 48, 49]. It is likely that as AHR ligands, these molecules directly
411 influence the epithelial/immune cell axis. For example, Zelante et al. showed that IAld drives AHR-
412 dependent IL-22 production and mucosal protection. Others have shown that innate lymphoid cell AHR
413 responses to be protective in inflammation through the production of IL-22 [16]. It is also noteworthy that
414 intraepithelial lymphocytes localize in response to AHR stimulation by dietary ligands [50], including
415 specific $CD4^{+}CD8\alpha\alpha^{+}$ subsets of intraepithelial T cells [51]. The activity of AHR ligands on intestinal
416 epithelia is less well understood. Similar to indole metabolites, we recently demonstrated that other
417 tryptophan-derived metabolites, including kynurenine, regulate epithelial IL-10R1 activity in an AHR-
418 dependent manner [23]. Such activity was associated with protection in colitis models and promoted
419 epithelial wound healing. These varied ligands suggest a promiscuous ligand-binding pocket of AHR that
420 is associated with agonistic activity [52]. Moreover, these results suggest redundant mechanisms to maintain
421 expression of functional epithelial IL-10 receptors, which have been shown to be essential for the
422 development and maintenance of barrier function [7].
423 Finally, it is known that colitis occurs as the result of immune cell responses to microbiota in
424 susceptible hosts [53]. These interactions are complex, involving multiple cell types and a spectrum of
425 metabolites. In this regard, we cannot rule out the contribution of cell types beyond the epithelium (e.g.
426 immune cells) in regulation by bacterial-derived metabolites in DSS. Rather, it is likely that these
427 metabolites have a plethora of actions on various cell types in the mucosa. In our studies, we have limited
428 this analysis to the epithelium to allow for a deeper and more mechanistic understanding of these
429 signaling responses. These studies provide strong evidence for the role of microbiota-derived indole

430 metabolites in anti-inflammatory pathways mediated by IL-10 signaling in the intestinal epithelium.
431 These findings present new insight to our understanding of host-microbial communication within the
432 mucosa and identify possible avenues for utilizing indoles as novel therapeutics in mucosal disease.
433

434 **Acknowledgements**

435 EEA, DJK, and SPC designed the study. EEA, JML, DJK, ELC, CJK, and KDB performed
436 experiments. MEG provided human serum samples. BRJ, STW, and DJK provided germ free mice,
437 human intestinal organoids and corresponding *in vitro* experiments. EEA and SPC wrote the manuscript,
438 all authors read and edited the manuscript. Thank you to Dr. Jason Spence and Sha Huang (University of
439 Michigan) for developing the human intestinal organoids from human pluripotent stem cells.
440
441
442
443
444
445
446
447
448
449
450
451
452
453
454

455 **References**
456

457 [1] Lozupone CA, Stombaugh JI, Gordon JI, Jansson JK, Knight R: Diversity, stability and resilience of
458 the human gut microbiota. Nature 2012, 489:220-30.

459 [2] Muniz LR, Knosp C, Yeretssian G: Intestinal antimicrobial peptides during homeostasis, infection,
460 and disease. Frontiers in immunology 2012, 3:310.

461 [3] Xavier RJ, Podolsky DK: Unravelling the pathogenesis of inflammatory bowel disease. Nature 2007,
462 448:427-34.

463 [4] Huttenhower C, Kostic AD, Xavier RJ: Inflammatory bowel disease as a model for translating the
464 microbiome. Immunity 2014, 40:843-54.

465 [5] Frank DN, St Amand AL, Feldman RA, Boedeker EC, Harpaz N, Pace NR: Molecular-phylogenetic
466 characterization of microbial community imbalances in human inflammatory bowel diseases. Proc Natl
467 Acad Sci U S A 2007, 104:13780-5.

468 [6] Engelhardt KR, Grimbacher B: IL-10 in humans: lessons from the gut, IL-10/IL-10 receptor
469 deficiencies, and IL-10 polymorphisms. Current topics in microbiology and immunology 2014, 380:1-18.

470 [7] Kominsky DJ, Campbell EL, Ehrentraut SF, Wilson KE, Kelly CJ, Glover LE, Collins CB, Bayless
471 AJ, Saeedi B, Dobrinskikh E, Bowers BE, MacManus CF, Muller W, Colgan SP, Bruder D: IFN-gamma-
472 mediated induction of an apical IL-10 receptor on polarized intestinal epithelia. J Immunol 2014,
473 192:1267-76.

474 [8] Colgan SP, Parkos CA, Matthews JB, D'Andrea L, Awtrey CS, Lichtman A, Delp C, Madara JL:
475 Interferon-γ induces a surface phenotype switch in intestinal epithelia: Downregulation of ion transport
476 and upregulation of immune accessory ligands. Am J Physiol 1994, 267:C402-C10.

477 [9] Kuhn R, Lohler J, Rennick D, Rajewsky K, Muller W: Interleukin-10-deficient mice develop chronic
478 enterocolitis. Cell 1993, 75:263-74.

479 [10] Chaudhry A, Samstein RM, Treuting P, Liang Y, Pils MC, Heinrich JM, Jack RS, Wunderlich FT,
480 Bruning JC, Muller W, Rudensky AY: Interleukin-10 signaling in regulatory T cells is required for
481 suppression of Th17 cell-mediated inflammation. Immunity 2011, 34:566-78.

482 [11] Wikoff WR, Anfora AT, Liu J, Schultz PG, Lesley SA, Peters EC, Siuzdak G: Metabolomics
483 analysis reveals large effects of gut microflora on mammalian blood metabolites. Proc Natl Acad Sci U S
484 A 2009, 106:3698-703.

485 [12] Zelante T, Iannitti RG, Cunha C, De Luca A, Giovannini G, Pieraccini G, Zecchi R, D'Angelo C,
486 Massi-Benedetti C, Fallarino F, Carvalho A, Puccetti P, Romani L: Tryptophan catabolites from
487 microbiota engage aryl hydrocarbon receptor and balance mucosal reactivity via interleukin-22. Immunity
488 2013, 39:372-85.

489 [13] Hubbard TD, Murray IA, Bisson WH, Lahoti TS, Gowda K, Amin SG, Patterson AD, Perdew GH:
490 Adaptation of the human aryl hydrocarbon receptor to sense microbiota-derived indoles. Scientific reports
491 2015, 5:12689.

492 [14] Mascanfroni ID, Takenaka MC, Yeste A, Patel B, Wu Y, Kenison JE, Siddiqui S, Basso AS,
493 Otterbein LE, Pardoll DM, Pan F, Priel A, Clish CB, Robson SC, Quintana FJ: Metabolic control of type
494 1 regulatory T cell differentiation by AHR and HIF1-alpha. Nature medicine 2015, 21:638-46.

495 [15] Kimura A, Naka T, Nohara K, Fujii-Kuriyama Y, Kishimoto T: Aryl hydrocarbon receptor regulates
496 Stat1 activation and participates in the development of Th17 cells. Proceedings of the National Academy
497 of Sciences of the United States of America 2008, 105:9721-6.

498 [16] Monteleone I, Rizzo A, Sarra M, Sica G, Sileri P, Biancone L, MacDonald TT, Pallone F,
499 Monteleone G: Aryl hydrocarbon receptor-induced signals up-regulate IL-22 production and inhibit
500 inflammation in the gastrointestinal tract. Gastroenterology 2011, 141:237-48, 48 e1.

501 [17] Gaitanis G, Magiatis P, Stathopoulou K, Bassukas ID, Alexopoulos EC, Velegraki A, Skaltsounis
502 AL: AhR ligands, malassezin, and indolo[3,2-b]carbazole are selectively produced by Malassezia furfur
503 strains isolated from seborrheic dermatitis. The Journal of investigative dermatology 2008, 128:1620-5.

504 [18] Vlachos C, Schulte BM, Magiatis P, Adema GJ, Gaitanis G: Malassezia-derived indoles activate the
505 aryl hydrocarbon receptor and inhibit Toll-like receptor-induced maturation in monocyte-derived
506 dendritic cells. The British journal of dermatology 2012, 167:496-505.

507 [19] McCracken KW, Howell JC, Wells JM, Spence JR: Generating human intestinal tissue from
508 pluripotent stem cells in vitro. Nat Protoc 2011, 6:1920-8.

509 [20] Pfaffl MW: A new mathematical model for relative quantification in real-time RT-PCR. Nucleic
510 acids research 2001, 29:e45.

511 [21] Albrecht E, Waldenberger M, Krumsiek J, Evans AM, Jeratsch U, Breier M, Adamski J, Koenig W,
512 Zeilinger S, Fuchs C, Klopp N, Theis FJ, Wichmann HE, Suhre K, Illig T, Strauch K, Peters A, Gieger C,
513 Kastenmuller G, Doering A, Meisinger C: Metabolite profiling reveals new insights into the regulation of
514 serum urate in humans. Metabolomics : Official journal of the Metabolomic Society 2014, 10:141-51.

515 [22] Dieleman LA, Palmen MJ, Akol H, Bloemena E, Pena AS, Meuwissen SG, Van Rees EP: Chronic
516 experimental colitis induced by dextran sulphate sodium (DSS) is characterized by Th1 and Th2
517 cytokines. Clin Exp Immunol 1998, 114:385-91.

518 [23] Lanis JM, Alexeev EE, Curtis VF, Kitzenberg DA, Kao DJ, Battista KD, Gerich ME, Glover LE,
519 Kominsky DJ, Colgan SP: Tryptophan metabolite activation of the aryl hydrocarbon receptor regulates
520 IL-10 receptor expression on intestinal epithelia. Mucosal Immunol 2017.

521 [24] Spence JR, Mayhew CN, Rankin SA, Kuhar MF, Vallance JE, Tolle K, Hoskins EE, Kalinichenko
522 VV, Wells SI, Zorn AM, Shroyer NF, Wells JM: Directed differentiation of human pluripotent stem cells
523 into intestinal tissue in vitro. Nature 2011, 470:105-9.

524 [25] Suzuki A, Hanada T, Mitsuyama K, Yoshida T, Kamizono S, Hoshino T, Kubo M, Yamashita A,
525 Okabe M, Takeda K, Akira S, Matsumoto S, Toyonaga A, Sata M, Yoshimura A: CIS3/SOCS3/SSI3
526 plays a negative regulatory role in STAT3 activation and intestinal inflammation. J Exp Med 2001,
527 193:471-81.

528 [26] Hubbard TD, Murray IA, Perdew GH: Indole and Tryptophan Metabolism: Endogenous and Dietary
529 Routes to Ah Receptor Activation. Drug Metab Dispos 2015, 43:1522-35.

530 [27] Lo R, Matthews J: High-resolution genome-wide mapping of AHR and ARNT binding sites by
531 ChIP-Seq. Toxicol Sci 2012, 130:349-61.

532 [28] Mathieu MC, Lapierre I, Brault K, Raymond M: Aromatic hydrocarbon receptor (AhR).AhR nuclear
533 translocator- and p53-mediated induction of the murine multidrug resistance mdr1 gene by 3-
534 methylcholanthrene and benzo(a)pyrene in hepatoma cells. J Biol Chem 2001, 276:4819-27.

535 [29] Lee JH, Wood TK, Lee J: Roles of indole as an interspecies and interkingdom signaling molecule.
536 Trends Microbiol 2015, 23:707-18.

537 [30] Manichanh C, Borruel N, Casellas F, Guarner F: The gut microbiota in IBD. Nat Rev Gastroenterol
538 Hepatol 2012, 9:599-608. .

539 [31] Butto LF, Haller D: Dysbiosis in intestinal inflammation: Cause or consequence. Int J Med
540 Microbiol 2016, 306:302-9. .

541 [32] Sartor RB: Microbial influences in inflammatory bowel diseases. Gastroenterology 2008, 134:577-94.

542 [33] Kominsky DJ, Keely S, MacManus CF, Glover LE, Scully M, Collins CB, Bowers BE, Campbell EL,
543 Colgan SP: An endogenously anti-inflammatory role for methylation in mucosal inflammation identified
544 through metabolite profiling. Journal of immunology (Baltimore, Md : 1950) 2011, 186:6505-14.

545 [34] Newton WA, Snell EE: Catalytic Properties of Tryptophanase, a Multifunctional Pyridoxal
546 Phosphate Enzyme. Proc Natl Acad Sci U S A 1964, 51:382-9.

547 [35] Hopkins FG, Cole SW: A contribution to the chemistry of proteids: Part II. The constitution of
548 tryptophane, and the action of bacteria upon it. J Physiol 1903, 29:451-66.

549 [36] Lee JH, Lee J: Indole as an intercellular signal in microbial communities. FEMS Microbiol Rev 2010,
550 34:426-44. .

551 [37] Martin K, Morlin G, Smith A, Nordyke A, Eisenstark A, Golomb M: The tryptophanase gene cluster
552 of Haemophilus influenzae type b: evidence for horizontal gene transfer. J Bacteriol 1998, 180:107-18.

553 [38] De Preter V, Machiels K, Joossens M, Arijs I, Matthys C, Vermeire S, Rutgeerts P, Verbeke K:
554 Faecal metabolite profiling identifies medium-chain fatty acids as discriminating compounds in IBD. Gut
555 2015, 64:447-+.

556 [39] Wlodarska M, Luo C, Kolde R, d'Hennezel E, Annand JW, Heim CE, Krastel P, Schmitt EK, Omar
557 AS, Creasey EA, Garner AL, Mohammadi S, O'Connell DJ, Abubucker S, Arthur TD, Franzosa EA,
558 Huttenhower C, Murphy LO, Haiser HJ, Vlamakis H, Porter JA, Xavier RJ: Indoleacrylic Acid Produced
559 by Commensal Peptostreptococcus Species Suppresses Inflammation. Cell Host Microbe 2017, 22:25-37
560 e6.

561 [40] Machiels K, Joossens M, Sabino J, De Preter V, Arijs I, Eeckhaut V, Ballet V, Claes K, Van
562 Immerseel F, Verbeke K, Ferrante M, Verhaegen J, Rutgeerts P, Vermeire S: A decrease of the butyrate-
563 producing species Roseburia hominis and Faecalibacterium prausnitzii defines dysbiosis in patients with
564 ulcerative colitis. Gut 2013.

565 [41] Eeckhaut V, Machiels K, Perrier C, Romero C, Maes S, Flahou B, Steppe M, Haesebrouck F, Sas B,
566 Ducatelle R, Vermeire S, Van Immerseel F: Butyricicoccus pullicaecorum in inflammatory bowel disease.
567 Gut 2013, 62:1745-52.

568 [42] Sokol H, Seksik P, Furet JP, Firmesse O, Nion-Larmurier I, Beaugerie L, Cosnes J, Corthier G,
569 Marteau P, Dore J: Low counts of Faecalibacterium prausnitzii in colitis microbiota. Inflammatory bowel
570 diseases 2009, 15:1183-9.

571 [43] Shimada Y, Kinoshita M, Harada K, Mizutani M, Masahata K, Kayama H, Takeda K: Commensal
572 bacteria-dependent indole production enhances epithelial barrier function in the colon. PLoS One 2013,
573 8:e80604. .

574 [44] Venkatesh M, Mukherjee S, Wang H, Li H, Sun K, Benechet AP, Qiu Z, Maher L, Redinbo MR,
575 Phillips RS, Fleet JC, Kortagere S, Mukherjee P, Fasano A, Le Ven J, Nicholson JK, Dumas ME, Khanna
576 KM, Mani S: Symbiotic bacterial metabolites regulate gastrointestinal barrier function via the xenobiotic
577 sensor PXR and Toll-like receptor 4. Immunity 2014, 41:296-310. .

578 [45] Cheng J, Shah YM, Gonzalez FJ: Pregnane X receptor as a target for treatment of inflammatory
579 bowel disorders. Trends Pharmacol Sci 2012, 33:323-30. .

580 [46] Devlin AS, Marcobal A, Dodd D, Nayfach S, Plummer N, Meyer T, Pollard KS, Sonnenburg JL,
581 Fischbach MA: Modulation of a Circulating Uremic Solute via Rational Genetic Manipulation of the Gut
582 Microbiota. Cell Host Microbe 2016, 20:709-15.

583 [47] Machiels K, Joossens M, Sabino J, De Preter V, Arijs I, Eeckhaut V, Ballet V, Claes K, Van
584 Immerseel F, Verbeke K, Ferrante M, Verhaegen J, Rutgeerts P, Vermeire S: A decrease of the butyrate-
585 producing species Roseburia hominis and Faecalibacterium prausnitzii defines dysbiosis in patients with
586 ulcerative colitis. Gut 2013, 10:2013-304833.

587 [48] Heath-Pagliuso S, Rogers WJ, Tullis K, Seidel SD, Cenijn PH, Brouwer A, Denison MS: Activation
588 of the Ah receptor by tryptophan and tryptophan metabolites. Biochemistry 1998, 37:11508-15.

589 [49] Jin UH, Lee SO, Sridharan G, Lee K, Davidson LA, Jayaraman A, Chapkin RS, Alaniz R, Safe S:
590 Microbiome-Derived Tryptophan Metabolites and Their Aryl Hydrocarbon Receptor-Dependent Agonist
591 and Antagonist Activities. Molecular Pharmacology 2014, 85:777-88.

592 [50] Li Y, Innocentin S, Withers DR, Roberts NA, Gallagher AR, Grigorieva EF, Wilhelm C, Veldhoen
593 M: Exogenous stimuli maintain intraepithelial lymphocytes via aryl hydrocarbon receptor activation. Cell
594 2011, 147:629-40.

595 [51] Cervantes-Barragan L, Chai JN, Tianero MD, Di Luccia B, Ahern PP, Merriman J, Cortez VS,
596 Caparon MG, Donia MS, Gilfillan S, Cella M, Gordon JI, Hsieh CS, Colonna M: Lactobacillus reuteri
597 induces gut intraepithelial CD4+CD8alphaalpha+ T cells. Science 2017, 357:806-10. .

598 [52] Bessede A, Gargaro M, Pallotta MT, Matino D, Servillo G, Brunacci C, Bicciato S, Mazza EM,
599 Macchiarulo A, Vacca C, Iannitti R, Tissi L, Volpi C, Belladonna ML, Orabona C, Bianchi R, Lanz TV,
600 Platten M, Della Fazia MA, Piobbico D, Zelante T, Funakoshi H, Nakamura T, Gilot D, Denison MS,
601 Guillemin GJ, DuHadaway JB, Prendergast GC, Metz R, Geffard M, Boon L, Pirro M, Iorio A, Veyret B,
602 Romani L, Grohmann U, Fallarino F, Puccetti P: Aryl hydrocarbon receptor control of a disease tolerance
603 defence pathway. Nature 2014, 511:184-90.

[53] Belkaid Y, Hand TW: Role of the microbiota in immunity and inflammation. Cell 2014, 157:121-41.

628 **Figures Legends**

629 **Figure 1. Tryptophan metabolism is altered in murine and human colitis. (A)** Relative levels of
630 indole metabolites in serum and whole colon tissue of mice receiving either water or 3% DSS for 7 d.
631 Metabolites were measured by LC/MS and GC/MS analysis, n = 5 mice per treatment group. **(B)**
632 Condensed pathway of tryptophan metabolism to indole and indole derivatives. **(C)** EC-HPLC analysis of
633 indole metabolites in serum of mice receiving either water or 2.5% DSS for 9 d. **(D)** Concentrations of
634 indole metabolites in serum of mice receiving either water or 2.5% DSS for 9 d (H2O, n = 5; DSS, n = 10
635 mice). **(E)** Indole-3-propionic acid (IPA) levels in serum samples from healthy controls (Con; n = 20),
636 subjects with active ulcerative colitis (UC; n = 15) and subjects with UC in remission (Rem; n = 20)
637 profiled by EC-HPLC. Data presented as mean ± S.E.M. *$P < 0.05$, **$P < 0.01$, Student's *t*-test and one-
638 way ANOVA.

639

640 **Figure 2. Indole metabolites improve barrier formation and induce IL-10R1 on intestinal epithelia.**
641 **(A)** qPCR of IL-10R1 transcript levels in T84 cells treated with IPA or IAld at varying concentrations for
642 6 h. **(B)** HIOs treated with 1mM IPA over 24 h. **(C)** Western blot analysis of IL-10R1 levels in T84 cells
643 treated with IPA at varying concentrations for 6 h (+ ctrl: FICZ at 1 μM) or in response to 1 mM IAld
644 over 24 h. **(D)** Transepithelial electrical resistance (TEER) of T84 cells treated with IAld (1 μM), IL-10
645 (10 ng/ml), or a combination of both was measured over 72 h. Data shown are represented as the average
646 TEER ± S.E.M. of triplicate samples. **$P < 0.01$, compared to untreated cells, two-way ANOVA. **(E)**
647 qPCR of SOCS3 transcript in T84 cells treated with IAld for 12 h, followed by treatment with IL-10 for 6
648 h. Data are presented as mean ± S.E.M. of at least three independent experiments. *$P < 0.05$, ***$P <$
649 0.001, Student's t-test.

650

651 **Figure 3. IL-10R1 expression is not induced by cells lacking AHR binding partner ARNT.**
652 **(A)** Lentiviral shRNA-mediated knockdown of ARNT (shARNT) in T84 intestinal epithelial cells relative
653 to T84 cells containing a non-template control (shNTC). **(B)** Transcript levels of CYP1A1 and CYP1B1

654 by qPCR in shNTC and shARNT T84 cells following IAld treatment for 12 h. **(C)** qPCR analysis of IL-
655 10R1 expression in shNTC and shARNT T84 cells treated with 1 mM IAld for 24 h. **(D)** Western blot
656 analysis of IL-10R1 levels in ARNT knockdown T84 cells. Confluent monolayers of T84 cells were
657 treated with IAld for 24 h. Protein expression was quantified by densitometry **(E)** and normalized to β-
658 actin. **(F)** qPCR of IL-10R1 transcript levels in shNTC and shARNT T84 cells treated with AHR inhibitor
659 (AHRi, 10 μM), IAld (1 mM), or both for 24 h. Data is presented as mean ± S.E.M. of three independent
660 experiments. *$P < 0.05$, **$P < 0.01$, compared to untreated shNTC, Student's t-test.
661
662 **Figure 4. Bacterial indole production induces IL-10R1. (A)** Indole production test of cultures from *E.*
663 *coli* K12 wild-type (*WT*), *tnaA* and *tnaB* mutants; "+" indicates presence of indole. **(B)** EC-HPLC
664 chromatogram of supernatants collected from *E. coli* K12 *WT* and *E. coli* Δ*tnaA*. **(C)** T84 cells were
665 treated for 24 h with serially diluted supernatants from *E. coli WT or E. coli* Δ*tnaA* cultures grown to
666 stationary phase, followed by media replenishment (M: molecular marker; + ctrl: IFN-γ at 10 ng/ml).
667 Germ free mice were colonized with *E. coli WT* or *E. coli* Δ*tnaA* for 2 wk followed by euthanasia. **(D)**
668 Indole concentrations in cecal contents were validated by HPLC in vehicle and colonized mice, and **(E)**
669 RNA was extracted from colons for qPCR analysis of Il10r1 expression (PBS, n = 5; *E. coli WT*, n = 4; *E.*
670 *coli* Δ*tnaA*, n = 5). Data are presented as mean ± S.E.M. *$P < 0.05$, **$P < 0.01$, Student's t-test.
671
672 **Figure 5. IPA improves DSS colitis outcomes.** Eight- to ten-wk-old C57BL/6 mice were administered
673 water or 2.5% DSS ± IPA *ad libitum* for 9 d. DSS was then removed and mice were allowed to recover
674 for 2 d as predetermined prior to euthanasia. **(A)** Concentration of IPA in colons of mice receiving DSS ±
675 IPA for up to 9 d. **(B)** Colon length measured at time of euthanasia. **(C)** Representative H&E-stained
676 colonic sections isolated from H2O-treated, H_2O/IPA-treated, DSS-treated, and DSS/IPA-treated mice at
677 20X magnification. **(D)** Histologic score of H&E-colonic sections. Colon tissue was homogenized and
678 cytokines were measured in protein lysates by Mesoscale analysis [**(E)** IFN-γ; **(F)** TNF-α; and **(G)** IL-

679 1β]. Data are presented as mean ± S.E.M. *$P < 0.05$, **$P < 0.01$, ***$P < 0.001$, two-way ANOVA and
680 Student's t-test.
681
682 **Supplemental Figure S1. IPA upregulates IL-10R1 in DSS colitis.** Eight- to ten-wk-old C57BL/6 mice
683 were administered water or 2.5% DSS ± IPA *ad libitum* for 9 d. DSS was then removed and mice were
684 allowed to recover for 2 d as predetermined prior to euthanasia. **(A)** qPCR of Il10r1 transcript levels in
685 colon tissue. **(B)** IL-10 levels in colon tissue protein lysates were measured by Mesoscale analysis. n = 5-
686 10 mice/group. Data are presented as mean ± S.E.M. *$P < 0.05$
687
688 **Supplemental Figure S2. IPA induces AHR target genes *in vivo.*** Transcript levels of **(A)** Cyp1a1 and
689 **(B)** Cyp1b1 were measured in colon tissue of eight- to ten-wk-old C57BL/6 mice administered water or
690 2.5% DSS ± IPA *ad libitum* for 9 d. **(C)** Further, colon tissue levels of IL-6 were measured in protein
691 lysates by Mesoscale analysis. n = 5-10 mice/group. Data are presented as mean ± S.E.M. *$P < 0.05$
692
693
694
695
696
697
698
699
700
701
702
703

704 **Tables**

705 **Table 1.** Primer sequences for qPCR.

Gene	Forward Primer	Reverse Primer
hACTB	5'-CCTGGCACCCAGCACAAT-3'	5'-GCCGATCCACACGGAGTACT-3'
hHSPCB	5'-TCTGGGTATCGGAAAGCAAGCC-3'	5'-GTGCACTTCCTCAGGCATCTTG-3'
hIL10R1	5'-CACATCCTCCACTGGACACC-3'	5'-CAAGGTCACTGCGGTAAGGT-3'
hSOCS3	5'-GGCCACTCTTCAGCATCTC-3'	5'-ATCGTACTGGTCCAGGAACTC-3'
hCYP1A1	5'-ACCCGCCACCCTTCGACAGTTC-3'	5'-TGCCCAGGCGTTGCGTGAGAAG-3'
hCYP1B1	5'-CTGGCACTGACGACGCCAAGA-3'	5'-TGGTCTGCTGGATGGACAGC-3'
hMDR1	5'-AACGGAAGCCAGAACATTCC-3'	5'-AGGCTTCCTGTGGCAAAGAG-3'
mActb	5'-TACGGATGTCAACGTCACAC-3'	5'-AAGAGCTATGAGCTGCCTGA-3'
mIl10r1	5'-CCCATTCCTCGTCACGATCTC-3'	5'-TCAGACTGGTTTGGGATAGGTTT-3'

706

707

708

709

710

711

712

713

714

715

716

717

718

719 **Table 2.** Study participant demographics.

Characteristic	Control	UC Remission	Ulcerative Colitis
Number	20	20	15
Sex			
Male	11	12	13
Female	9	8	2
Age	58.6 ± 10.9	46.5 ± 18.6	40.4 ± 13.4
Disease Location			
Left-sided	n/a	6	1
Extensive	n/a	14	12
Proctitis	n/a	0	2

720

721

722

723

724

725

726

727

728

729

730

731

732

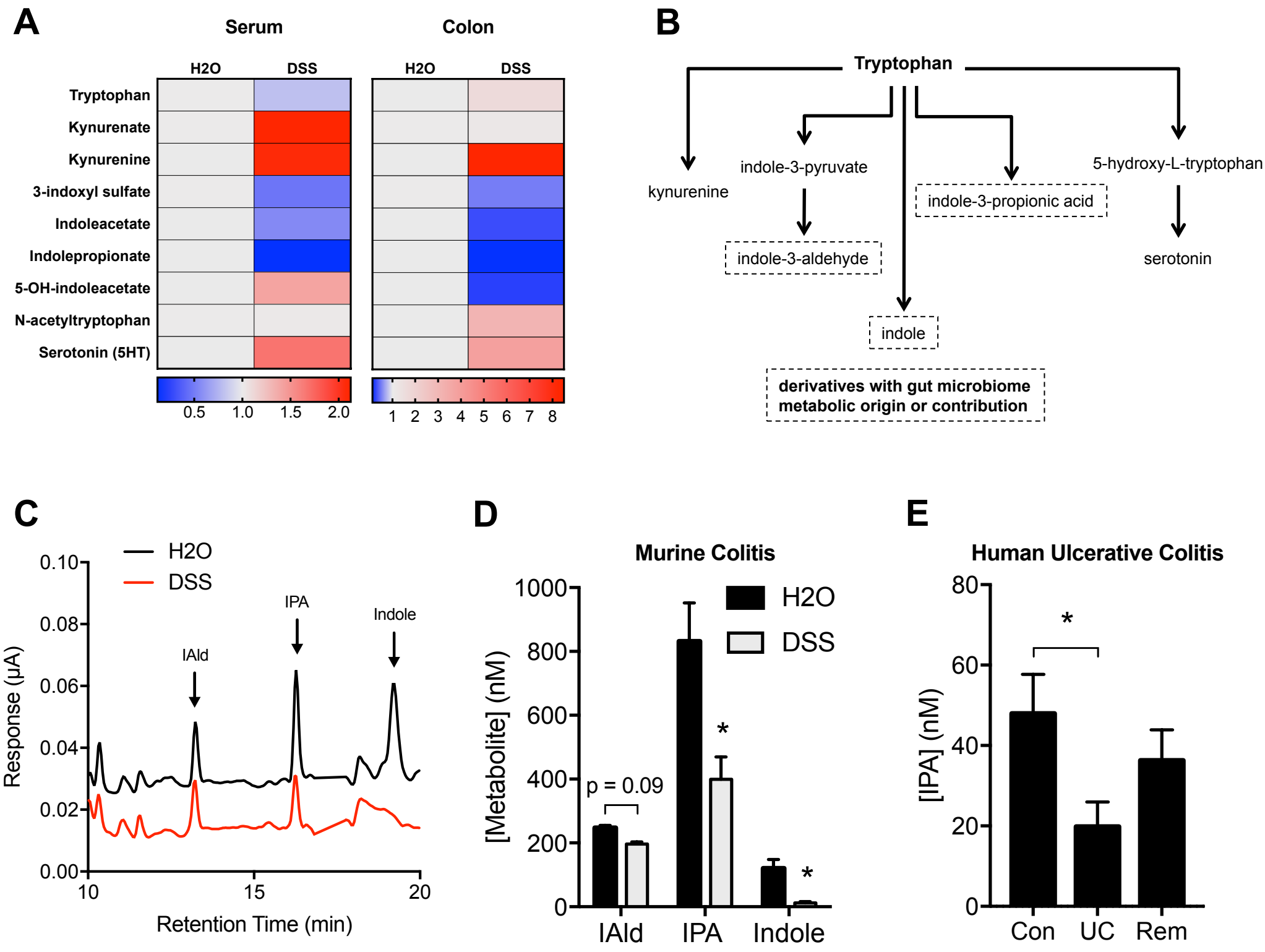
A
Serum
Colon
H2O
DSS
H2O
DSS
Tryptophan
Kynurenate
Kynurenine
3-indoxyl sulfate
Indoleacetate
Indolepropionate
5-OH-indoleacetate
N-acetyltryptophan
Serotonin (5HT)
0.5 1.0 1.5 2.0
1 2 3 4 5 6 7 8
B
Tryptophan
kynurenine
indole-3-pyruvate
indole-3-propionic acid
5-hydroxy-L-tryptophan
indole-3-aldehyde
serotonin
indole
derivatives with gut microbiome metabolic origin or contribution
C
H2O
DSS
IAld
IPA
Indole
Response (µA)
0.10
0.08
0.06
0.04
0.02
0.00
10
15
20
Retention Time (min)
D
Murine Colitis
H2O
DSS
[Metabolite] (nM)
1000
800
600
400
200
0
p = 0.09
*
*
IAld
IPA
Indole
E
Human Ulcerative Colitis
[IPA] (nM)
80
60
40
20
0
*
Con
UC
Rem

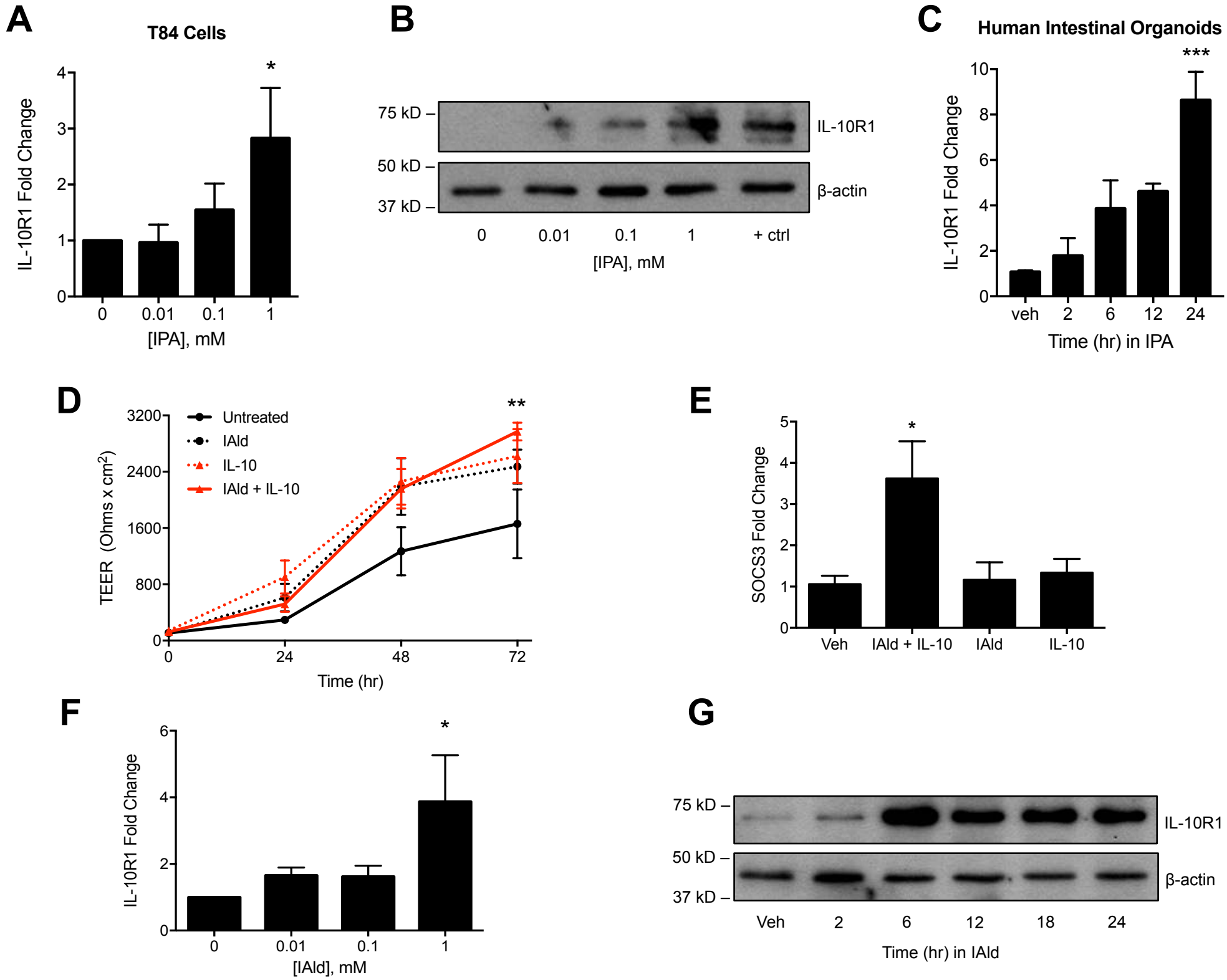
A
T84 Cells
IL-10R1 Fold Change
[IPA], mM
0
0.01
0.1
1
*
B
75 kD
50 kD
37 kD
IL-10R1
β-actin
0
0.01
0.1
1
+ ctrl
[IPA], mM
C
Human Intestinal Organoids
IL-10R1 Fold Change
***
veh
2
6
12
24
Time (hr) in IPA
D
Untreated
IAld
IL-10
IAld + IL-10
TEER (Ohms x cm2)
**
Time (hr)
E
SOCS3 Fold Change
*
Veh
IAld + IL-10
IAld
IL-10
F
IL-10R1 Fold Change
*
[IAld], mM
G
75 kD
50 kD
37 kD
IL-10R1
β-actin
Veh
2
6
12
18
24
Time (hr) in IAld

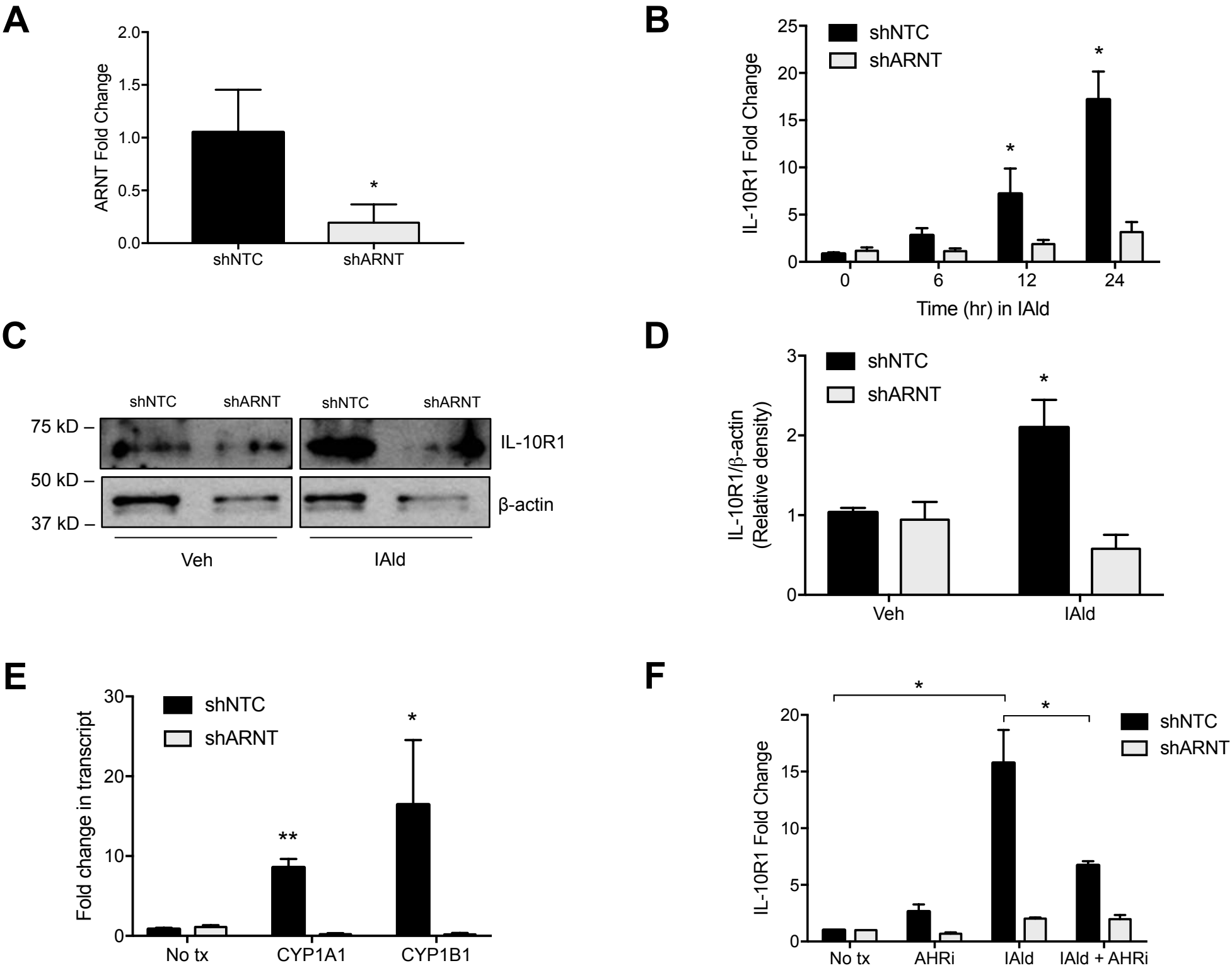
A
ARNT Fold Change
2.0
1.5
1.0
0.5
0.0
*
shNTC
shARNT
B
IL-10R1 Fold Change
25
20
15
10
5
0
shNTC
shARNT
*
*
0
6
12
24
Time (hr) in IAld
C
shNTC
shARNT
shNTC
shARNT
75 kD –
50 kD –
37 kD –
IL-10R1
β-actin
Veh
IAld
D
IL-10R1/β-actin
(Relative density)
3
2
1
0
shNTC
shARNT
*
Veh
IAld
E
Fold change in transcript
30
20
10
0
shNTC
shARNT
**
*
No tx
CYP1A1
CYP1B1
F
IL-10R1 Fold Change
20
15
10
5
0
*
*
shNTC
shARNT
No tx
AHRi
IAld
IAld + AHRi

A

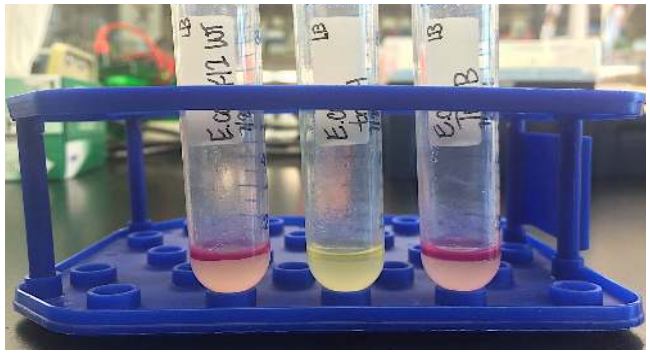

Strain:	*E. coli*^{WT}	*E. coli*$^{\Delta tnaA}$	*E. coli*$^{\Delta tnaB}$
Indole:	+	-	+

B

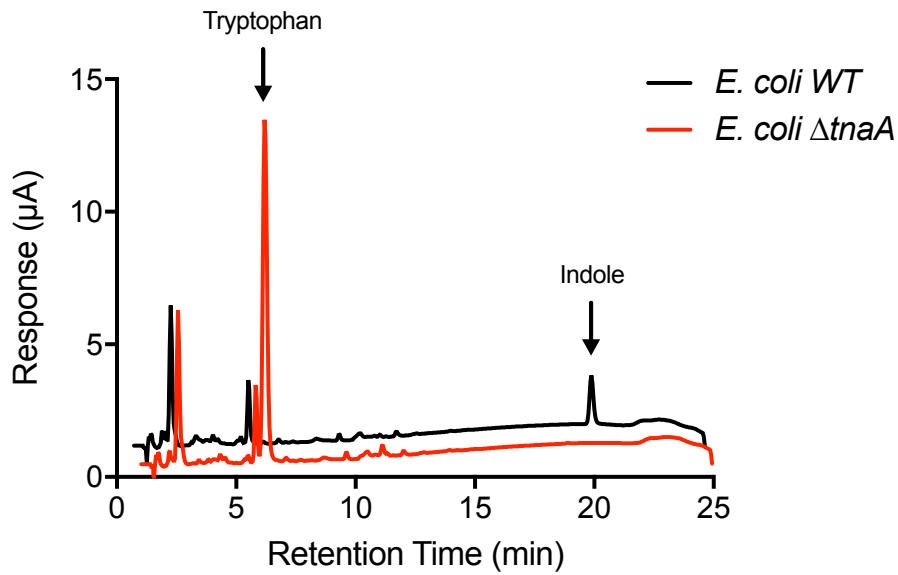

C

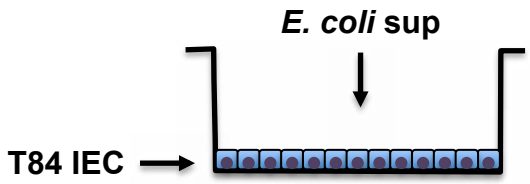

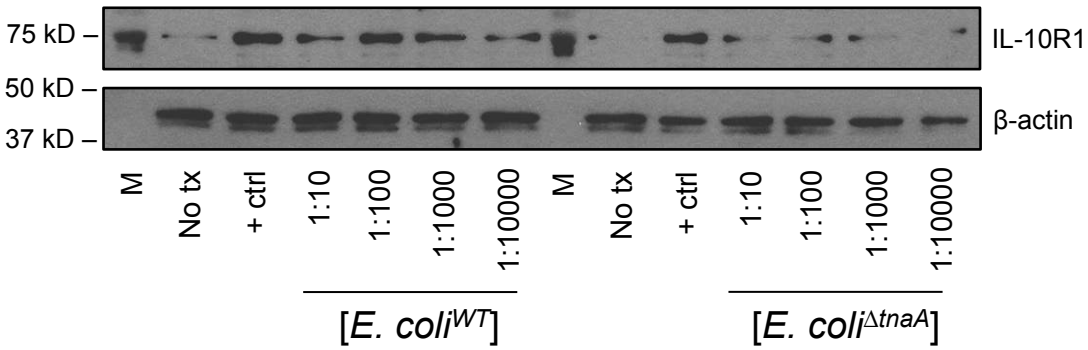

D

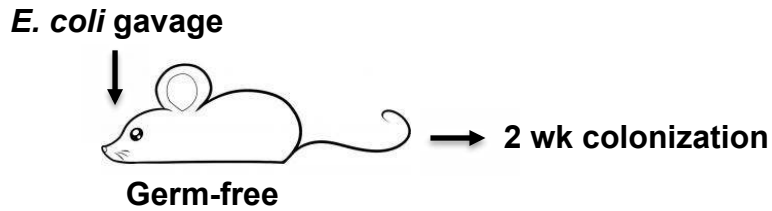

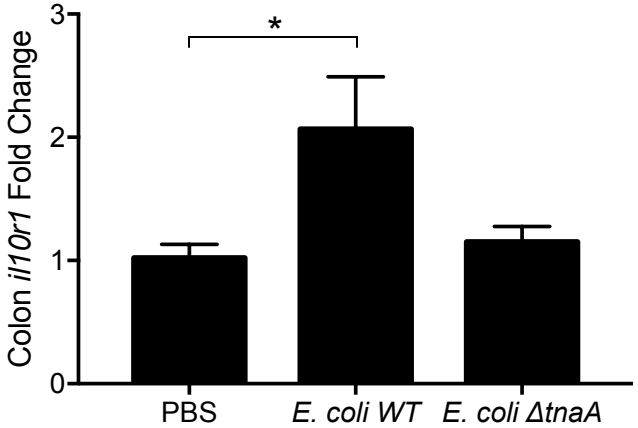

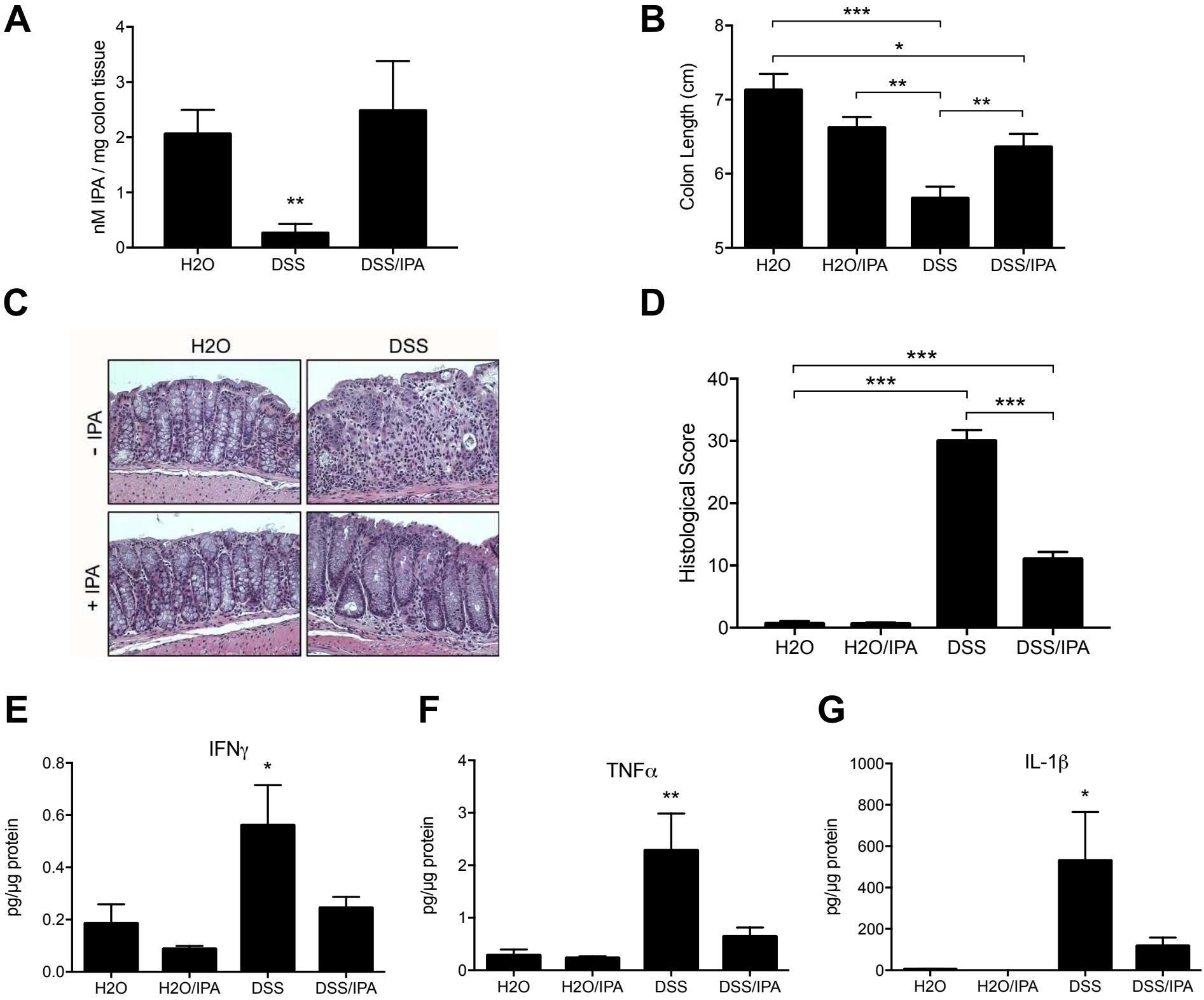
A
nM IPA / mg colon tissue
0
1
2
3
4
**
H2O
DSS
DSS/IPA
B
Colon Length (cm)
5
6
7
8
***
*
**
**
H2O
H2O/IPA
DSS
DSS/IPA
C
H2O
DSS
- IPA
+ IPA
D
Histological Score
0
10
20
30
40
***
***
***
H2O
H2O/IPA
DSS
DSS/IPA
E
IFNγ
pg/µg protein
0.0
0.2
0.4
0.6
0.8
*
H2O
H2O/IPA
DSS
DSS/IPA
F
TNFα
pg/µg protein
0
1
2
3
4
**
H2O
H2O/IPA
DSS
DSS/IPA
G
IL-1β
pg/µg protein
0
200
400
600
800
1000
*
H2O
H2O/IPA
DSS
DSS/IPA